https://doi.org/10.5194/nhess-2021-309
Preprint. Discussion started: 9 November 2021
© Author(s) 2021. CC BY 4.0 License.

Natural Hazards and Earth System Sciences
Open Access
Discussions

Modelling geographical and built environment's attributes as predictors of human vulnerability during tsunami evacuations: a multi-case study and paths to improvement

Jorge León[1,3], Alejandra Gubler[2,3], Alonso Ogueda[4]

[1]Department of Architecture, Universidad Técnica Federico Santa María, Valparaíso, Chile
[2]Department of Civil Engineering, Universidad Técnica Federico Santa María, Valparaíso, Chile
[3]National Research Center for Integrated Natural Disaster Management (CIGIDEN), Santiago, Chile
[4]Department of Mathematical Sciences, George Mason University, Virginia, United States

Correspondence to: Jorge León (jorge.leon@usm.cl)

Abstract. Evacuation is the most important and effective method to save human lives during a tsunami. In this respect, challenges exist in developing quantitative analyses of the relationships between the evacuation potential and the built environment and geographical attributes of coastal locations. This paper proposes a computer-based modelling approach (including inundation, evacuation, and built environment metrics), followed by multivariate regressive analysis, to estimate how those attributes might influence the expected tsunami death ratios of seven Chilean coastal cities. We obtained, for the examined variables, their average values to different thresholds of the death ratio. Also, our statistical analysis allowed us to compare the relative importance of each metric, showing that the maximum flood, the straightness of the street network, the total route length, and the travel time can have a significant impact on the expected death ratios. Moreover, we suggest that these results could lead to spatial planning guidelines for developing new urban areas into exposed territories (if this expansion cannot be restricted or discouraged) or retrofitting existing ones, with the final aim of enhancing evacuation and therefore increasing resilience.

1 Introduction

Tsunamis are relatively rare phenomena but capable of triggering widespread destruction and causing significant human casualties in exposed coastal areas. In the last two decades, devastating events, including those in Indonesia (2004, 2006, 2010, 2018), Samoa (2009), Chile (2010, 2014, 2015) and Japan (2011), provoked more than 250,000 deaths globally (WHO, 2021). Authorities and scholars have suggested and developed a range of countermeasures to reduce tsunami risk: 'hard' strategies like structural defences (e.g. sea walls and flood gates) and the construction of elevated ground, and 'soft' approaches focused on education and policy, like land-use and built-environment planning, plus early warning and emergency management systems (Suppasri et al., 2012b; Ting et al., 2015; Tsimopoulou et al., 2012). While 'hard' countermeasures are uncommon out of Japan, 'soft' planning-focused strategies require extended periods and high political

https://doi.org/10.5194/nhess-2021-309
Preprint. Discussion started: 9 November 2021
© Author(s) 2021. CC BY 4.0 License.
Natural Hazards and Earth System Sciences
Open Access
EGU
Discussions

and community support to be implemented. Typically, this is hard to achieve in developing countries like Indonesia and Chile, where hence community-focused emergency management, emphasising evacuation, is the most feasible strategy to reduce the vulnerability of populations to tsunamis. Moreover, there is a growing consensus on evacuation as the most important and effective method for saving human lives during a tsunami (Shuto, 2005; Suppasri et al., 2012b), which is particularly true in areas exposed to near-field events, with peak arrival times as short as 15 min.

In the context of disaster risk reduction policies and studies, 'risk' is habitually defined as the combination of 'hazard' and 'vulnerability' factors (e.g. Eckert et al., 2012; UNISDR, 2009; Wisner et al., 2012). The former focuses on how existing social, economic, infrastructural, and environmental conditions (within a defined spatial context and timespan) can be affected by an external threat (natural or man-made). The latter refers to that context's pre-event characteristics that create the potential for harm, including exposure, susceptibility, and coping aspects (Birkmann et al., 2010; Cutter et al., 2008; Turner et al., 2003). Authors like Birkmann (2006) and Frazier et al. (2014) stress the need for strengthening and focus risk mitigation and adaptation plans through the spatial assessment of hazard and vulnerability factors. In line with this, based on thorough analyses of previous tsunamis disasters' outcomes (including the 2011 Great Tohoku tsunami, the 2010 Chilean tsunami, the 2009 Samoan tsunami, and the 2004 Indian Ocean tsunami) or pre-disaster modelling, scholars like Anwar et al. (2011), Birkmann et al. (2010), Eckert et al. (2012), González-Riancho et al. (2015), Suppasri et al. (2016), and Zamora et al. (2021) have underlined a range of characteristics leading to tsunami risk (with a focus on either the population or the built environment). These aspects comprise indicators of hazard (e.g. tsunami height, flow depth and arrival time), exposure (e.g. elevation, shoreline distance, number of people exposed, population density, housing density, infrastructures, land use) and vulnerability (e.g. warning systems, governance and institutional arrangements, evacuation potential, economic resources, education, personal awareness/knowledge/decision-making capacity).

Several studies aim at quantitatively examining tsunami vulnerability and its correlation with geographical, built environment and socio-psychological features, within a spatially specific area or domain of study, from neighbourhoods to whole regions, including blocks, districts, cities, and metropolitan areas. For instance, as shown by Tarbotton et al. (2015), most researchers use post-tsunami destruction data to focus on built structures and develop statistically-based empirical vulnerability functions that model the damage response to tsunamis. A common type of function is the fragility curve, which combines the probability of damage (Y-axis) with hydrodynamic characteristics such as flood depth, flow velocity and force (X-axis). Typically, researchers develop these curves by integrating satellite remote sensing, numerical modelling of tsunami inundation, and post-tsunami survey data (examined in GIS systems) (Koshimura et al., 2009). In line with this, Suppasri et al. (2012a) (using data from the 2011 Great East Japan Earthquake and Tsunami) apply least squares regression to demonstrate how building characteristics like the structural material, number of stories and coastal topography can influence their damage levels. Other tsunami disasters examined through this approach include the 2010 Chilean Tsunami in Dichato (Mas et al., 2012) and the 2018 Sulawesi tsunami at Palu Bay in Indonesia (Mas et al., 2020). In the former, the researchers estimated the affected houses' structural fragility through a post-tsunami survey. They combined this with an interpolated inundation depth (developed in geographic information systems from measures taken in the field) to deliver a tsunami

https://doi.org/10.5194/nhess-2021-309
Preprint. Discussion started: 9 November 2021
© Author(s) 2021. CC BY 4.0 License.

fragility curve. In the case of the Sulawesi tsunami, the authors created the fragility functions by integrating field survey data, visual interpretation of satellite images, and machine learning for multi-sensor and multitemporal satellite images.

Other studies focus on quantitatively assessing human vulnerability to tsunamis and its possible explanatory factors. For instance, Goto and Nakasu (2018) use data from the 2011 Great East Japan Earthquake and Tsunami to propose a Human Vulnerability Index (HVI) that combines each location's fatality rate and the rate of incidence of washed-out buildings. Moreover, they apply multivariate regressive analysis to identify four explanatory variables for this index: (1) Allowance period (the tsunami arrival time divided by the distance to a safe place; (2) Preparedness (the rate of affected evacuees for analysis who had prepared emergency carry-out bags beforehand); (3) Road serviceability (the rate of car-using evacuees × car speed); and (4) Warning effect (multiplication of announced tsunami height and cognition rate of warning). Yavuz et al. (2020) use probabilistic tsunami modelling (developed from earthquake databases from 1900–2013) to evaluate social, economic and environmental risks on the Eastern Mediterranean coast. Specifically, they define social risk as to the number of people in areas where inundation depth reaches 0.5 m or higher. In turn, working with the case of the 2004 tsunami disaster in Banda Aceh, Indonesia, Koshimura et al. (2009) used regressive analysis to develop a fragility function for human death ratio through the combination of tsunami modelling and post-tsunami data. This function used the number of dead, missing, and saved residents in 88 examined villages, plus the modelled inundation depth. Nateghi et al. (2016) analysed municipality-level and sub-municipality-level data from the 1896, 1933, 1960, and 2011 tsunamis that affected the Tohoku area in Japan. With this information, they worked out a model based on statistical learning methods that allowed them to appraise the effectiveness of seawalls and coastal forests in mitigating destruction and death rates provoked by tsunamis.

In cases where tsunamis have not occurred recently or their data is not available, researchers typically use computer-based models to estimate human vulnerability according to simulated scenarios. For instance, Sugimoto et al. (2003) developed a tsunami human damage prediction method for Usa town, Tosa City, Shikoku Island, Japan, in the context of a possible Nankai earthquake to occur during the first half of the 21st century. Their method comprised a GIS-based spatial model integrating tsunami numerical modelling, exposed populations, and expected evacuation behaviours (e.g. departure times) obtained from questionnaire surveys. This model delivered the predicted loss of human lives in 3 different scenarios, depending on the tsunami hazard factors (over 0.5 m inundation depth or more than 2.0 m/s flow velocity) and evacuation behaviour (with or without evacuation activities). In line with this, evacuation modelling has been extensively used in recent years to estimate human casualties during tsunami scenarios, using both 'dynamic' and 'static' approaches (Imamura et al., 2012). Models couple expected evacuation performances with discrete or probabilistic tsunami floods to estimate mortality rates across evacuees. Examples of 'dynamic' evacuation models include, for instance, agent-based (León et al., 2019a; Makinoshima et al., 2016; Mostafizi et al., 2017; Taubenböck et al., 2009; Wang et al., 2016; Wang and Jia, 2020) and cellular automata (e.g. Kitamura et al., 2020). In turn, GIS-based, least-cost-distance (Wood et al., 2018, 2020) and network approaches (Dewi, 2012; González-Riancho Calzada et al., 2013) are examples of 'static' evacuation models, which allow the identification of 'evacuation landscapes' (Wood et al., 2014).

As Goto and Nakasu (2018) point out, a quantitative analysis of the relationships between fatalities rates and geographical, built environment, and socio-psychological features can support the development of effective measures to reduce the loss of human lives. Moreover, if place-based models' findings can be generalised, this "will produce a tool for measuring areal vulnerability to future tsunamis and enable municipalities to prioritise the order of their countermeasures" (Goto and Nakasu, 2018, p.2). In the case of evacuation as a method for reducing tsunami vulnerability, Mohareb (2011) points out that three main factors determine the evacuees' behaviour, which in turn relate to a broad number of geographical and socio-psychological aspects: (1) social behaviour (i.e. how the evacuees will psychologically react in a crowd during an emergency); (2) spatial behaviour (i.e. the selection of the escape routes and the required time for evacuation); and (3) the characteristics of the evacuation phase (i.e. human response time, travel time, and waiting time). While socio-psychological aspects can be critical determinants of evacuation (see, for instance, Perry et al. (1981) and Murray-Tuite and Wolshon (2013)), we will focus our research on some of the most relevant attributes of the geographical and built environments (capable of being quantitatively assessed through computer-based modelling) that could contribute to the success (or failure) of evacuation in the case of a tsunami. These characteristics include those related to the tsunami (flood depth), context (elevation, distance to the shoreline), the evacuation process (travel time, distance to the shelter, route length, pedestrian directness ratio), and the street network configuration (betweenness, closeness, straightness). In this respect, authors like Allan et al. (2013), Kubisch et al. (2020), Tumini et al. (2017), Villagra et al. (2014), and Villagra and Quintana (2017) underline the links between urban morphology/geospatial characteristics and evacuation. They point out how the former physically affects the latter and examine how behavioural aspects (e.g. the decision of evacuation, route selection or evacuation mode) relate to the environmental factors. In line with this, following Goto and Nakasu (2018), we aim at quantitatively assessing the relationship between geographical and built environments' attributes and tsunami vulnerability (represented by the expected death ratio) as a first step towards the proposal of evidence-based countermeasures for risk reduction. For instance, as most evacuations take place in cities, planners and decision-makers could apply our recommendations for built environment changes and standards (aimed at increasing the number of evacuees that can reach safe areas) to guide the physical development retrofitting of tsunami-prone coastal communities around the world. This, with the final aim of enhancing pedestrian evacuation, saving lives, and therefore increasing resilience.

León et al. (2021) deliver a modelling framework (including flood and agent-based evacuation) to examine the relationship between the evacuation potential and urban form characteristics of 67 urban samples from 12 case studies in Chile. In turn, they use the model's outcomes to develop a multivariate regressive analysis, which allows them to 'weight' the relative importance of each of the independent variables (i.e. the urban form characteristics) on the evacuation times. In this paper, we propose to enhance their approach with a greater emphasis on the description of real-world geographical and built environment conditions that might influence tsunami evacuation. Therefore, while León et al. (2021) set up a generic tsunami scenario where they test selected urban samples for flood and evacuation, we aim at developing a multi-case study approach that encompasses real-world-based large flood and evacuation models for seven coastal cities in Chile: Arica, Iquique, Coquimbo, La Serena, Viña del Mar, Valparaíso, and Talcahuano (see Fig. 1). Moreover, we focus our descriptive

https://doi.org/10.5194/nhess-2021-309
Preprint. Discussion started: 9 November 2021
© Author(s) 2021. CC BY 4.0 License.

and multivariate regressive analyses on the expected death ratios of these cities' exposed areas (as an indicator of human vulnerability to tsunamis) and how they can be affected by the geographical and built environment characteristics.

The rest of this paper is as follows. Section 2 describes the methodology, which comprises the selection of the seven examined Chilean cities and a description of two scaffolding cross-case research phases: a descriptive statistical analysis and a multivariate regressive analysis. Section 3 presents the results of our research, which we discuss in section 4. Lastly, section 5 delivers the study's main findings and proposes paths for future investigation.

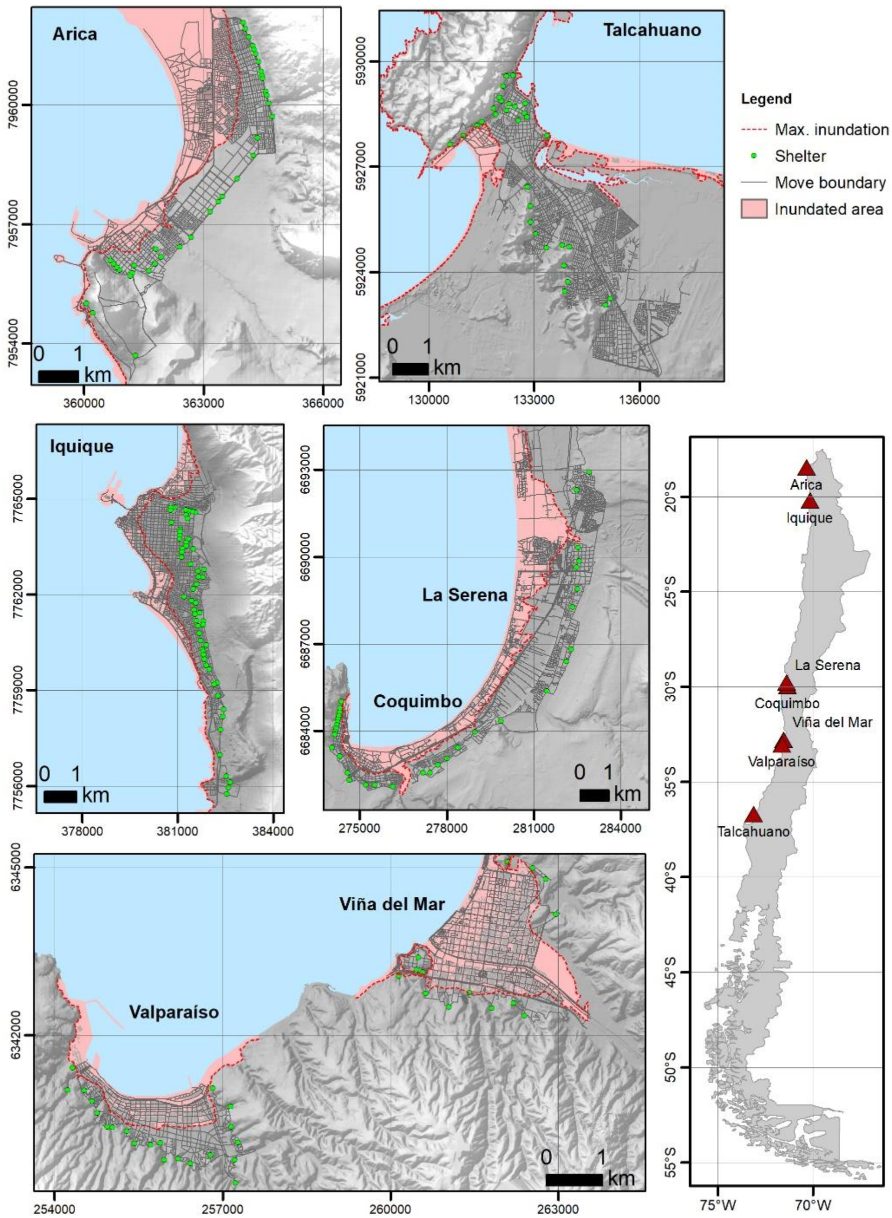

Fig. 1: Location and evacuation-related features of the examined case studies in Chile.

https://doi.org/10.5194/nhess-2021-309
Preprint. Discussion started: 9 November 2021
© Author(s) 2021. CC BY 4.0 License.
Natural Hazards and Earth System Sciences
Discussions

2 Methodology

2.1 Case studies

Chile is one of the most tsunami-prone countries globally, with more than 100 tsunamis recorded since the 16th century, including 35 destructive events (Lagos and Gutiérrez, 2005) and recent disasters in 2010, 2014 and 2015. Moreover, researchers including Drápela et al. (2021), Klein et al. (2017), and Medina et al. (2021) have underlined the existence of extensive submarine areas in seismic locking along the central and northern coasts of Chile, capable of triggering large destructive tsunamis if major rupture earthquakes occur. Among the Chilean coastal cities, we selected seven case studies, distributed from north to south: Arica, Iquique, Coquimbo, La Serena, Viña del Mar, Valparaíso, and Talcahuano (see Fig. 1). According to the Chilean Bureau of Statistics (INE), these cities are among the top-20 in Chile with the most significant ratios of exposed populations to tsunamis (INE, 2021). This information is based on census data and the official tsunami flood charts by SHOA (the Chilean Navy's agency aimed to provide technical elements, information and technical assistance to offer navigational safety in Chilean waters) (SHOA, 2012). Talcahuano, Iquique, and Arica occupy the first three places in the list, with 43.01%, 29.77%, and 23.44% of their populations living in floodable areas, respectively. In each of these cities we focused our analysis only on inhabited areas. Overall, the seven case studies gather roughly 240,000 exposed residents. As seen in Table 1, historical records (since the 16th century) show that destructive tsunamis have systematically affected these cities.

Case study	Location	Total population (census 2017)	Exposed resident population (CITSU)	Ratio of exposed resident population (%)	Years of recorded destructive tsunamis	Modelled population for evacuation (daytime scenario, departure time = 8 min)	Source of daytime population	Total number of 4x4 m. cells	Number of 'lethal' 4x4 m. cells
Arica	Northern Chile	221,364	51,888	23.44	1604, 1868, 1877	81,420	Call Detail Records (CDR) provided by Movistar (May 8, 2019, between 10:00 and 11:00)	52,358	11,159
Iquique	Northern Chile	191,468	57,000	29.77	1604, 1868, 1877, 2014	109,891	Origin-destination study by	108,689	32,296

https://doi.org/10.5194/nhess-2021-309
Preprint. Discussion started: 9 November 2021
© Author(s) 2021. CC BY 4.0 License.

Natural Hazards and Earth System Sciences
Discussions

							SECTRA (2014)		
La Serena	Northern Chile	221,054	19,939	9.02	1849, 1922, 2015	172,631	Call Detail Records (CDR) provided by Movistar (January 19, 2019, between 22:00 and 24:00)	211,451	20,844
Coquimbo	Northern Chile	227,730	6,240	2.74					
Viña del Mar	Central Chile	334,248	35,096	10.5	1730, 1822	62,519	Origin-destination study by SECTRA (2016)	37,859	20,592
Valparaíso	Central Chile	296,655	4,450	1.5	1730, 1822	32,492	Origin-destination study by SECTRA (2016)	16,063	7,038
Talcahuano	Southern Chile	151,749	65,267	43.01	1570, 1657, 1751, 1835, 1868, 2010	34,996	Call Detail Records (CDR) provided by Movistar (May 8, 2019, between 10:00 and 11:00)	103,671	774

Table 1: Attributes of the examined case studies in Chile.

2.2 Descriptive analysis

This phase aimed to develop a thorough description of the current geographical and built environment conditions that might influence the outcome of tsunami evacuations in each of the case studies and, second, to integrate those results through GIS spatial post-processing based on 4x4m. cells as the basic units of study.

https://doi.org/10.5194/nhess-2021-309
Preprint. Discussion started: 9 November 2021
© Author(s) 2021. CC BY 4.0 License.

2.2.1 Tsunami inundation and evacuation models

We developed coupled tsunami inundation and evacuation models for each case study, using the methodologies extensively described in León et al. (2019b) and León et al. (2020). First, we worked out flood simulations according to the worst-case feasible seismic scenario (i.e. a high consequence event of a relatively small likelihood (Løvholt et al., 2014)) for each city. To do this, we used the Storm Surge and Tsunami Simulator in Oceans and Coastal Areas (STOC), specifically the Multi-layered Static Dynamics Model (STOC-ML) (Tomita et al., 2006). We used seismic models by Carvajal et al. (2017) and Fujii and Satake (2012), and for the Iquique scenario we calculated the seismic parameters, including length, width, and slip, according to the scaling law by Papazachos et al. (2004) (see Table 2). The input data for the simulations included bathymetry, coastline, topography, and elevation data, compiled from various sources including SHOA, local governments and GEBCO (www.gebco.net). Each case study's simulation used five nested grids for numerical analysis, with spatial resolutions of 1,536, 256, 32, 8 and 4 m, respectively. Tsunamis were simulated for 45 minutes (comprising its development from the occurrence of the earthquake to the maximum inland penetration, i.e. the inundation line or run-up). The model used a time step of 0.1 s, also recording time series, the inundation depth (every 10 min), and the maximum inundation depth.

Case study	**Mw**	**Total length [km]**	**Total width [km]**	**Slip [m]**	**Source**	**Description**
Arica	9.0	600	150	Uniform slip 17.0 [m]	Own	Large earthquake and tsunami
Iquique	8.5-8.7	500	160	Variable slip with peak of 10.0 [m]	Matías Carvajal	As a result of the accumulated slip since 1877
Coquimbo, La Serena, Valparaíso and Viña del Mar	9.1-9.3	600	180	Variable slip with peak of 19.7 [m]	Carvajal et al. (2017)	The 1730 Valparaíso Earthquake
Talcahuano	8.8	See the Fujii and Satake (2012) model for the Maule 2010 earthquake, developed from tsunami and coastal geodetic data				

Table 2: Seismic parameters of the examined case studies.

We also developed agent-based evacuation simulations for each case study, using an enhanced version of the PARI-AGENT model (Arikawa, 2015). Agent-based models are bottom-up computer simulations where individual disaggregated elements (the agents, which in our model correspond to evacuees) are modelled as autonomous decision-making entities that follow simple rules, which are iteratively performed within a set time threshold, usually including stochastic features. The agents' interactions (also with their environment) lead to emergent phenomena, which is helpful for the examination of complex, real-life events like mass evacuation (Mas et al., 2015; Mostafizi et al., 2017). To develop the agent-based models for each case study, we had to follow these steps.

First, we included the inundation parameters obtained from the STOC-ML analyses. Second, we determined the evacuation territories of each case study (henceforth denominated 'move boundary', see Fig. 1), comprising the streets and open spaces connecting the coastline with the safe assembly areas (shelters) as defined by the evacuation plans from ONEMI, the Chilean Emergency Management Agency (available at https://geoportalonemi.maps.arcgis.com/apps/webappviewer/index.html?id=5062b40cc3e347c8b11fd8b20a639a88). For their spatial definition, these move boundaries used the smallest nested grid from the inundation model (with 4x4m. cells). We obtained their specific configuration through its intersection with the street network obtained from OpenStreetMap (https://www.openstreetmap.org/) and post-processed in ArcMap 10.4.1 (see Fig. 1). Third, we had to establish worst-case daytime population distributions (different from census data), reflecting that most of the examined zones comprise downtown, CBD, or touristic areas that significantly increase their populations during daytime due to commuting and visiting (see Table 1). In the case of Iquique, Viña del Mar, and Valparaíso, we obtained daytime populations from previous origin-destination studies conducted by the Chilean Ministry of Transportation (SECTRA, 2014, 2016). For Arica, Coquimbo, La Serena, and Talcahuano, in turn, we used extrapolations of mobile CDR (call detail records) databases provided by one of the largest telecom companies in Chile (with a market share of roughly 28%). In the case of Arica and Talcahuano, we used the morning peak time (10:00 to 11:00) of a random weekday (May 8, 2019) as the worst-case daytime scenario. For Coquimbo and La Serena, popular summer touristic destinations with vibrant nightlife along their coastlines, we used Saturday, January 19, 2019, between 22:00 and 24:00. The PARI-AGENT code randomly distributed these populations across the move boundaries within each case study (locating one or more agents on each 4x4 m. cell). Fourth, we established the agents' performance parameters, including: (1) the impact of the slope on the evacuees' speed, according to Tobler's exponential hiking function (Tobler, 1993); (2) a Rayleigh probabilistic distribution of departure times for evacuees (with a mean time = 8 min, which corresponds to the average time that ONEMI takes to release an evacuation warning); (3) an evacuation speed for each agent, according to its age (Buchmueller and Weidmann, 2006), probabilistically defined based the case studies' population pyramids from the 2017 Census (INE, 2018); (4) a random-walk parameter that introduces an aleatory fluctuation up to 10º on the evacuation direction; and (5) a crowd potential parameter that makes the agent tend to follow the direction in which other evacuees are moving, stochastically assigned (with a probability of 0.5). Fifth, we executed the simulation, in which the code initially computes the optimal route for each agent, according to its initial position and closest shelter, using the A* algorithm (Yao et al., 2010). Then, it calculates every agent's position at each time step (1 s), based on its departure time and velocity (which could be modified by the slope, random-walk and crowd parameters). The code compares this new position with the water height at that moment (obtained from the inundation file) and updates the agent's status: (1) moving (i.e., alive), (2) dead (i.e., reached by the water), or (3) escaped (i.e., alive in the shelter). This process continues for 45 min. and then the computation stops.

https://doi.org/10.5194/nhess-2021-309
Preprint. Discussion started: 9 November 2021
© Author(s) 2021. CC BY 4.0 License.

As the model included stochastic parameters (the initial positions of the agents, their walking speeds and departure times, and the random-walk factor), we carried out at least ten simulation rounds for each case study, intending to achieve a 95% confidence interval with a margin of error <1% in the average values of the number of escaped, moving and dead evacuees after 45 min. The model also recorded each agent's travel time and evacuation route (for every iteration).

2.2.2 Street network configuration model

According to Fakhrurrazi and Van Nes (2012), an appropriate street network configuration can increase the evacuees' chances of successfully evacuating in case of a tsunami. The suitability of a street network for evacuation depends on factors like its accessibility, variety of route options and the possibility of short, direct trips (Dill, 2004; Handy et al., 2003). While a range of metrics has been proposed to examine these characteristics (Sharifi, 2019), we will focus our analysis on centrality indicators, which can be used "to measure the degree of importance of specific nodes/links in a street network" (Sharifi, 2019, p.174), based on how central the locations are compared to the rest of the urban layout (Porta et al., 2006). Moreover, centrality is a good predictor of everyday human movement (Sasabe et al., 2020; Turner, 2007), and authors like Mohareb (2011) and Marín Maureira and Karimi (2017) point out that evacuees tend to choose well-known paths instead of the designated ones.

We examined the move boundaries (described in section 2.2.1 above) from each case study with the Urban Network Analysis Toolkit for ArcMap (UNA) (Sevtsuk et al., 2013). For each street segment belonging to the input network, we analysed three centrality metrics: (1) betweenness, (2) straightness, and (3) closeness. These can be defined, respectively, as (Sevtsuk et al., 2013; Sharifi, 2019): (1) the fraction of shortest paths between all pairs of destinations in the street network that pass through an examined street segment; (2) the extent to which the shortest paths from a segment of interest to all the other segments in the street network resemble straight Euclidean paths; and (3) an indication of how close a street segment is to all other street segments in the network. To compare the street network's components, the toolkit normalises the outcomes according to the total number of segments in the network. The Urban Network Analysis Toolkit delivers its outputs as a new GIS vector shapefile, with the input street network including these metrics.

2.2.3 Context-determined evacuation metrics

Each discrete location belonging to the examined areas of each case study (represented in our model by a 4x4 m. cell) has a set of evacuation metrics determined by its existing spatial relationships to the geographical and built contexts. We examined these metrics using ArcMap 10.4.1 and the same data sources mentioned in sections 2.2.3 and 2.2.4 above. These indicators include (1) elevation; (2) sea distance, i.e. the straight-line distance between the cell's centre and its closest shoreline point; (3) distance to shelter, i.e. the straight-line distance between the cell's centre and the closest safe assembly area; and (4) pedestrian directness ratio (PDR) (also termed "Pedestrian Route Directness, (PRD)" by Dill (2004)), which is the ratio of the 'real-world' route distance (as determined by the street network) and the straight-line distance connecting the cell's centre and its closest safe assembly area. In this respect, Hillier and Iida (2005) and Hillier (2009) underline that the strongest movement predictor is the least angle change along the routes. Therefore, networks including fewer direction changes (i.e., lower PDR values) might improve the evacuees' wayfinding performance. Wayfinding is "the process of determining and following a path or route between an origin and a destination" (Allen, 1999, p.6).

2.2.4 Spatial post-processing

In this research phase, we aimed to integrate the previous sections' outcomes into a descriptive spatial analysis that could also serve as the basis for the subsequent multivariate regressive study. We carried out this integration with the aid of the ArcMap 10.4.1 software. Our canvas included the move boundaries described in section 2.2.1 above for each case study, which comprised a network of streets and open spaces represented by raster files with 4x4 m. cells. Each of these cells corresponded to a specific location in the evacuation landscape, for which all the calculated metrics had to be spatialised. First, as the inundation and agent-based models used the same base raster, the former's results did not need to be post-processed. Second, the data from each case study's evacuation model included a range of at least ten different groups of agents' initial locations (each with an associated final status: moving, dead, or escaped). Due to our purpose of examining vulnerability, we aimed at quantifying, for each cell, its death ratio (i.e. the percentage of dead agents that began their journey from it, comprising all the model's iterations). To do this, we used the ArcMap's Spatial Join Tool, which joined the attributes from the source feature (i.e. the initial locations of agents, all merged in a single shapefile) to the target feature (i.e. the raster-based street network). Third, for the case of the street configuration model, we applied the same Spatial Join tool to cast the properties from the outcoming street network into the base raster. Lastly, as we also calculated the context-determined evacuation metrics on the base raster, their results did not need to be post-processed, either.

Our analysis, comprising all the case studies, included 530,091 cells, each of them containing 12 data fields: death ratio, mean travel time, sea distance, shelter distance, elevation, total route length, estimated arrival time (ETA) of the maximum flood, maximum flood, betweenness, closeness, straightness, and pedestrian directness ratio (PDR)). Table 1 shows the number of examined cells for each case study.

2.3 Multivariate regressive analysis

For each case study, the result from the spatial post-processing was a raster shapefile representing the evacuation territory, where each cell included the 12 data fields mentioned in section 2.2.4. The objective of our regressive analysis was to test, for each of the 530,091 cells, the death ratio (the dependent variable) against the other 11 independent variables, which represent characteristics of the geography and built environment. In this way, we could examine how much each of these characteristics contributes to the expected death ratios. To do this, we developed a multivariate regressive analysis using a random forest methodology, which combines a multitude of simp decision trees or tree predictors at training time. Random forest models segment independent variables in random regions to adjust prediction (Breiman, 2001).

We applied a K-Fold cross-validation method to assess this model's outcomes (Mosteller and Tukey, 1968). Following this method, we randomly split all the input data (comprising the 12 variables) into five equal-size packages (folds). In four of

https://doi.org/10.5194/nhess-2021-309
Preprint. Discussion started: 9 November 2021
© Author(s) 2021. CC BY 4.0 License.

them (the training packages), we applied our regressive random forest model to internally predict the values of the death ratio, according to the independent variables; this was the 'training' test. We repeat this process for the 'external' fifth package (the testing one) on the 'testing' test. Then, we calculated the coefficient of determination (R2) to assess the strength of the relationship between the predicted and actual dependent in the 'training' and 'testing' packages. After that, we tried the other four combinations of training and testing packages to obtain further R2 scores. Then, we executed other five random splits of the input data, leading to overall 30 repetitions of the procedure. Overall, our mean R2 scores were 0.9101 (SD=0.0021) and 0.8607 (SD=0.0022) for the 'training' and 'testing' analyses, respectively, which underline our model's goodness-of-fit. Lastly, to enhance the interpretation of the model's results, we used SHAP values. These aim at assessing (for every cell) how much has each independent variable contributed to the prediction of the death ratio, compared to the average prediction of this dependent variable across all the cells (Lundberg and Lee, 2017).

To develop our statistical analysis, we used an ad-hoc Python model, comprising the data analysis libraries NumPy (Berg et al., 2020) (https://numpy.org/), pandas (McKinney et al., 2020) (https://pandas.pydata.org/), and SHAP (Lundberg, 2020) (https://github.com/slundberg/shap).

3 Results

3.1 Death ratios and the natural and built environment's characteristics

Table 3 summarises our descriptive analysis comprising 530,091 cells belonging to the case studies' move boundaries. This table arranges the data in 11 intervals according to growing (in 10% steps) death ratio thresholds. For each of these intervals, we include the mean values of 11 data fields (mean travel time, sea distance, shelter distance, elevation, total route length, estimated arrival time (ETA) of the maximum flood, maximum flood, betweenness, closeness, straightness, and pedestrian directness ratio (PDR)). Figure 2, in turn, compares these results between the case studies, using normalised values for the independent variables (based on the highest record for each of them), for three death ratio thresholds: 0, greater than 0, and 1.

Death ratio thresholds	**Mean travel_time (sec.)**	**Sea distance (m.)**	**Shelter distance (m.)**	**Elevation (m.a.s.l.)**	**Total route length (m.)**	**Estimated arrival time (ETA) of the maximum flood (sec.)**	**Maximum flood depth (m.)**	**Betweenness**	**Closeness**	**Straightness**	**Pedestrian directness ratio**	**Number of examined cells**
0	922.60	1185.38	675.08	13.82	910.11	49.16	0.61	1358067.32	9.88632E-07	36494.23	1.40	437,388
>0.0	858.13	296.57	1107.70	5.39	1419.89	364.76	4.67	602292.98	1.53525E-06	20874.97	1.36	92,703
>0.1	839.00	295.93	1123.30	5.61	1452.12	354.02	5.13	415711.57	1.42721E-06	15255.32	1.37	65,353
>0.2	832.36	307.76	1133.97	5.89	1464.85	316.78	5.34	282384.39	1.2593E-06	11463.28	1.36	50,383
>0.3	827.92	312.69	1147.21	5.99	1478.09	296.55	5.50	200697.99	1.15586E-06	9444.16	1.35	42,245

https://doi.org/10.5194/nhess-2021-309
Preprint. Discussion started: 9 November 2021
© Author(s) 2021. CC BY 4.0 License.

>0.4	820.13	310.76	1161.72	5.99	1492.13	281.72	5.59	150408.25	1.10805E-06	8388.61	1.35	35,542
>0.5	799.21	295.33	1177.81	5.87	1508.79	282.44	5.66	114267.89	1.08333E-06	7668.96	1.34	28,329
>0.6	786.67	299.90	1189.45	5.88	1526.85	282.08	5.81	102126.81	1.03059E-06	7337.72	1.34	23,536
>0.7	776.61	300.71	1195.04	5.87	1530.47	268.94	5.82	94337.01	1.00919E-06	7332.52	1.33	19,888
>0.8	774.60	310.38	1193.33	5.91	1526.73	247.92	5.80	93960.46	9.83519E-07	7420.44	1.33	16,754
>0.9	785.42	326.40	1171.41	6.02	1499.34	216.67	5.70	96782.60	9.28422E-07	7686.08	1.3	14,753
1	797.02	337.88	1150.73	6.09	1476.24	191.53	5.58	99491.43	8.93807E-07	7945.43	1.3	13,825

Table 3: Death ratio thresholds and average values of the independent variables.

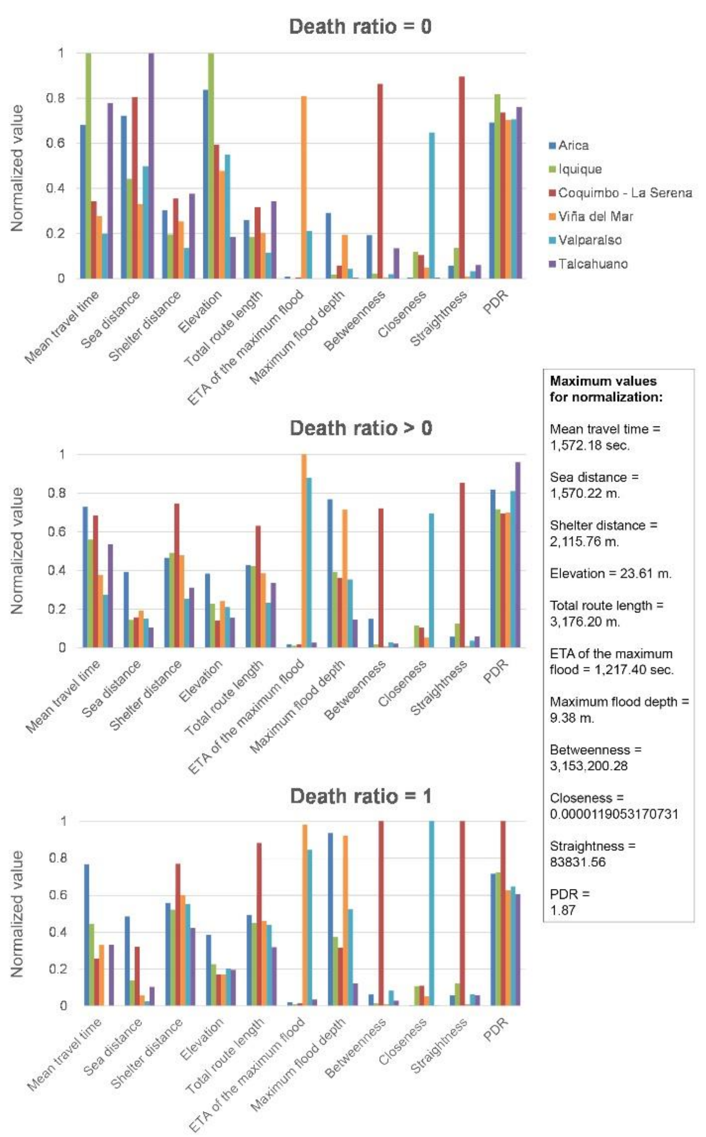

Fig. 2: Case studies comparison of the normalised average values of the 11 independent variables for three different death ratio thresholds: 0, >0 and 1.

https://doi.org/10.5194/nhess-2021-309
Preprint. Discussion started: 9 November 2021
© Author(s) 2021. CC BY 4.0 License.
Natural Hazards and Earth System Sciences
Open Access
Discussions

3.2 Multivariate regressive analysis

Figures 3 and 4 show the results of the SHAP values analysis for the Random Forest model's outcomes. Figure 3 shows, for every independent variable and all the examined cells, the amount of the former's contribution (either positive or negative) to the predicted death ratio (compared to the average prediction across all the cells). Red dots mean higher values of the independent variable, while blue ones imply the opposite. Figure 4 processes this data to display, for each independent variable, the average absolute contribution to the predicted death ratio.

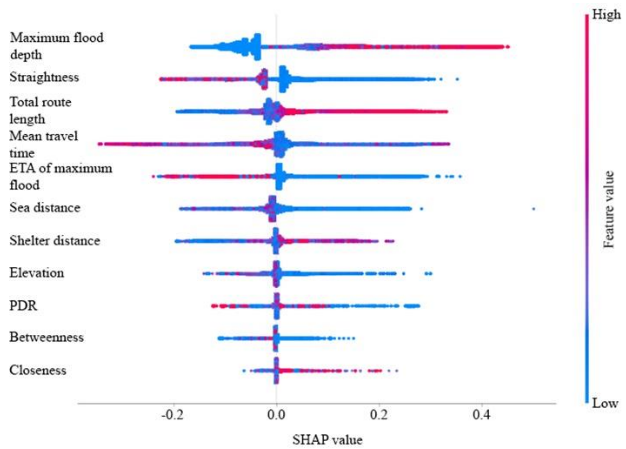

Fig. 3: SHAP values of the independent variables

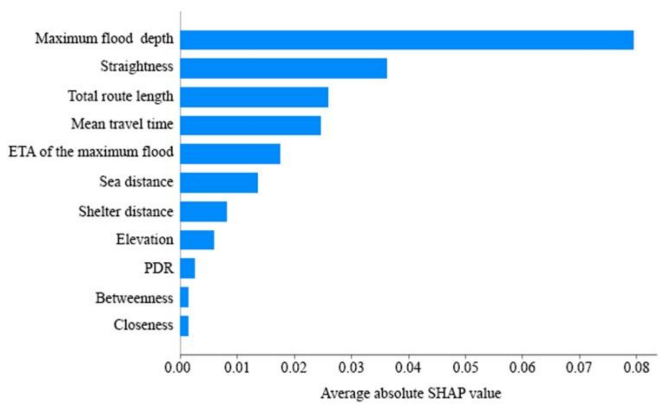

Fig. 4: Average absolute SHAP values of the independent variables

4 Discussion

Our descriptive analysis included 530,091 cells. Of these, 92,703 (17.49%) have a death ratio > 0 (i.e. at least one agent from any of the model's run, who started its evacuation from one of them, was caught by the tsunami). In turn, 13,825 cells (2.61%) have a death ratio = 1, which means that the waters reach every agent departing from them before arriving at a safe assembly area. As shown by Table 1 and Fig. 2, the rate of cells with elevated death ratios is unevenly distributed across the case studies. Cities like Viña del Mar, Valparaíso, and Iquique show large percentages of cells susceptible to having dead evacuees (54.78%, 43.81%, and 29.71%, respectively). On the contrary, Talcahuano has barely 0.74% of its cells on this condition. As we can see in the maps include in Fig. 1, while the first three cities gather considerable urban development and residential populations on exposed locations right next to the coastline, most of the last one's territory is roughly 1.0 to 1.5 km from the coast, from whom large, marshy areas separate it.

The death ratio thresholds included in Table 3 allow appraising, for the examined case studies, how each independent variable relates to the possibility of death in case of a tsunami. On the one hand, 8 of the 11 examined variables exhibit an expected behaviour: the differences between the average values of the 'safe' (death ratio = 0) and 'lethal' (death ratio > 0) cells are significant in the case of the shelter distance, maximum flood, total route length, sea distance, elevation,

https://doi.org/10.5194/nhess-2021-309
Preprint. Discussion started: 9 November 2021
© Author(s) 2021. CC BY 4.0 License.

betweenness, straightness, and pedestrian directness ratio (PDR). In the first three of them, the death ratio increases when they augment; in the other five, their decreases imply higher death ratios.

On the other hand, three variables show somewhat counterintuitive results: the death ratio increases when the mean travel time reduces, and when the estimated arrival time (ETA) of the maximum flood, and the closeness, grow. In the case of the first of these independent variables, the results are likely influenced by the fact that the evacuees departed from 'lethal' cells have comparatively shorter evacuation times, as the tsunami soon reaches them and cannot complete their evacuation paths. In the case of the street network's closeness (which is a measure of how close a cell is to all other cells in the 'evacuation territory'), one may expect that more compact street networks should lead to shorter evacuation routes (and times) and, therefore, less 'dead' evacuees. Nevertheless, according to our results, it would be possible that these smaller networks are faster to flood by the incoming tsunami. Lastly, in the case of the ETA, it is essential to underline that the estimated arrival time of the maximum flood is not necessarily the same as the onset time of the first tsunami front. In our model, the latter can have much more impact on the evacuees' survival rates.

While tsunamis and their related evacuation potentials are highly context-dependent, our cross-case results could serve to identify and appraise other tsunami-vulnerable areas in Chile. Moreover, they highlight possible spatial planning guidelines that could be applied to develop new urban regions into exposed territories (if this expansion cannot be restricted or discouraged). For instance, our results show that the average number of tsunami-caused deaths would occur across those evacuees initially located within an approximately 300-meters-wide buffer zone from the coastline. In line with this, Løvholt et al. (2014, p.133) point out that studies of the impact of the 2004 Indian Ocean Tsunami show that "in Sri Lanka, people within the 100-m zone from the shoreline were more likely to die and to be seriously injured than people living outside this zone". In turn, González-Riancho et al. (2015) underline that 72% of the housing units within the 200-m line from the shoreline in Sri Lanka were completely or partially damaged, leading to a higher number of victims. Eckert et al. (2012) also point out that buildings within that area are highly vulnerable. In the case of the tsunami flood, while inundation depths can be above 10 meters at several of our case studies' coastlines, our model shows that the average flood depth at the 'lethal' departure cells is roughly 4.67 m. In turn, 'safe' cells have a comparatively low mean value of 0.61 m, implying that some evacuees can avoid being caught by the advancing tsunami front if they rapidly leave the floodable areas. These results are in line with the literature on human casualties during past tsunamis. For instance, Suppasri et al. (2016) point out that the inundation depths that increased fatality ratios during the 2011 Great East Japan Tsunami are primarily around 10 or 5 m., depending on the specific geographical characteristics of different examined areas. In line with this, Murakami et al. (2012) examined the human loss distribution during the 2011 disaster in Yuriage District, Natori City, showing that inundation depths between 1.87 m. and 8.50 m. triggered death ratios up to 22.3%. In turn, in the case of the ground elevation, the average value of the 'safe' cells is 13.82 m. When we include 'lethal' cells in the analysis, we can see that fatalities concentrate around elevations of six meters and below. In this respect, Eckert et al. (2012) argue that buildings located at a height of 5-10 m. can be considered of medium vulnerability to tsunamis, while those with an elevation above ten m. have low vulnerability. For the previously mentioned case of the Yuriage District, Murakami et al. (2012) report elevations less

Natural Hazards and Earth System Sciences
Open Access
EGU
Discussions

than five m. in the deadly areas. It is also noticeable that cells belonging to street networks with good integration levels, that also allow short walks to the safe assembly areas, and have few direction changes (i.e. with high betweenness, straightness and PDR values, respectively), have lower death ratios. In this respect, as Sharifi (2019) underlines, locations with high betweenness centrality values can easily lead to many other sites within the network. Therefore, it is critical to maintaining their functionality during disasters.

To focus on possible paths to improvement for these case studies is helpful to examine the outcomes from our multivariate regressive analysis. In this respect, as shown by Fig. 3 and 4, some independent variables have comparatively higher impacts on the death ratios as predicted by our regressive model. The most significant one is the maximum flood, followed by the straightness, the total route length, and the travel time. The maximum flood levels on 'lethal' cells are difficult to mitigate unless hardware-type defences are built (which, as mentioned above, is unlikely in developing countries like Chile). Moreover, we already pointed out that the tsunami flood also conditions the travel time in our regressive analysis. Nevertheless, the straightness and total route length depend on real-world urban configurations, resulting from the case studies' historical development process. They hence can be subject to strategic interventions to modify their values to reduce the cells' death ratios. In this respect, more direct routes are not only faster to walk (thus reducing escape distances and evacuation times) but also help to improve wayfinding as they reduce the changes of directions that evacuees must undertake between their origins and destinations (Fakhrurrazi and Van Nes, 2012; Mohareb, 2011). The importance of wayfinding cannot be underestimated, especially in the case of tourists and non-locals, who may constitute a large percentage of casualties during a tsunami (as shown by the Chilean disaster of 2010) (Kubisch et al., 2020). Also, the total route length (and the shelter distance) could also be reduced by incorporating vertical evacuation across the urban fabric, which has been proven to reduce the evacuation times significantly (León et al., 2019a; Mostafizi et al., 2019). Currently, vertical evacuation in Chile is recommended as only a second choice of escape if horizontal evacuation is not feasible (ONEMI, 2014).

Thorough evacuation analyses are context-dependent and must take care of geographical and socio-psychological aspects (Mohareb, 2011; Murray-Tuite and Wolshon, 2013; Perry et al., 1981). In this respect, one limitation of our study is that the latter are not analysed. Moreover, research on socio-psychological determinants of tsunami evacuation could help to critically review some of our model's central assumptions (e.g. a 'full compliance' evacuation, the probabilistically distributed departure times, or the routing process). Nevertheless, our analysis provides a significant step into identifying and examining geographical and built environment's attributes that might influence the evacuation potential of coastal communities, as a spatial framework for the subsequent analysis of their specific socio-psychological characteristics.

5 Conclusion

- We proposed a modelling-based approach (including inundation, evacuation, and urban form metrics) to quantitatively appraise, through statistical regressive analysis, some of the most relevant aspects of the geographical and built environments that could contribute to the success (or failure) of evacuation in the case of a tsunami, using a cross-case study of seven Chilean coastal cities.

- According to our results, some of these cities can have up to roughly 55% of their move boundaries (i.e. the evacuation area between the coastline and the safe inland assembly areas) susceptible to having dead evacuees.
- We also demonstrated that geographical, urban form and evacuation variables, including the maximum flood, straightness, total route length, and travel time, could significantly impact the expected death ratios in each case study. Moreover, we describe the average values of these metrics related to different thresholds of death ratio.
- We argued that, while engineered countermeasures to control flood levels are unlikely in developing countries like Chile, urban form metrics like the street network's straightness could be the subject of improvements through planning processes. Moreover, this would allow other enhancements in other evacuation dimensions like the travel time and evacuees' wayfinding.
- Future research could enhance our approach with the incorporation of socio-psychological aspects and probabilistic tsunami flood modelling. Also, more case studies (at both the national and global levels) could help test our findings' robustness and generalizability.

Data availability

DBF files compressing the post-processed spatial data can be downloaded from: https://usmcl-my.sharepoint.com/:f:/g/personal/jorge_leon_usm_cl/Emfj8ZYFmb1EhZmQ49dbLJ4Bi5z1HOvc-TKHsg0Wg5GZBw?e=KAL2Z5

Author contribution

Jorge León: conceptualisation, methodology and writing – original draft. Alejandra Gubler: tsunami and evacuation modelling, review and editing. Alonso Ogueda: statistical modelling.

Competing interests

The authors declare that they have no conflict of interest.

Acknowledgments

This research was funded by the research grant ANID/FONDECYT n◦ 11170024, and by the National Research Center for Integrated Natural Disaster Management (CIGIDEN), ANID/FONDAP/ 15110017. It was also supported by the supercomputing infrastructure of the NLHPC (ECM-02). We also thank Matías Carvajal for providing the fault model of the Iquique earthquake.

References

Allan, P., Bryant, M., Wirsching, C., Garcia, D. and Rodriguez, M. T.: The Influence of Urban Morphology on the Resilience of Cities Following an Earthquake, J. Urban Des., 18(2), 242–262, 2013.

Allen, G. L.: Spatial Abilities, Cognitive Maps, and Wayfinding. Bases for individual differences in spatial cognition and behavior., in Wayfinding Behavior. Cognitive mapping and other spatial processes, edited by R. Golledge, pp. 46–80, The John Hopkins University Press, Baltimore., 1999.

Anwar, H., Gebert, N., Mueck, M., Muhari, A., Post, J., Stein, E., Wegscheider, S., Birkmann, J., Riedlinger, T. and Strunz, G.: GUIDELINE FOR TSUNAMI RISK ASSESSMENT IN INDONESIA. SCIENTIFIC PROPOSAL FOR PRACTITIONER AND END USERS. [online] Available from: https://www.gitews.org/tsunami-kit/en/E1/further_resources/GITEWS Guideline for Tsunami Risk Assessment in Indonesia.pdf (Accessed 10 July 2019), 2011.

Arikawa, T.: Development of High Precision Tsunami Simulation Based on a Hierarchical Intelligent Simulation, in Proceedings of the 34th JSST Annual International Conference on Simulation Technology, Toyama, Japan., 2015.

Berg, S., Fernández del Río, J., Gommers, R., Haldane, A., Harris, C., Hoyer, S., Picus, M., Smith, N., Taylor, J., Virtanen, P., van der Walt, S. and Wieser, E.: NumPy, [online] Available from: https://numpy.org/ (Accessed 11 January 2021), 2020.

Birkmann, J.: Indicators and criteria for measuring vulnerability: Theoretical bases and requirements, in Measuring Vulnerability to Natural Hazards : Towards Disaster Resilient Societies, pp. 55–77, United Nations University Press, Tokyo, JP., 2006.

Birkmann, J., Teichman, K. v., Welle, T., González, M. and Olabarrieta, M.: The unperceived risk to Europe's coasts: tsunamis and the vulnerability of Cadiz, Spain, Nat. Hazards Earth Syst. Sci., 10(12), 2659–2675, doi:10.5194/nhess-10-2659-2010, 2010.

Breiman, L.: Random forests, Mach. Learn., 45(1), 5–32, doi:10.1023/A:1010933404324, 2001.

Buchmueller, S. and Weidmann, U.: Parameters of pedestrians, pedestrian traffic and walking facilities, Institute for Transport Planning and Systems, ETH Zürich, Zürich., 2006.

Carvajal, M., Cisternas, M. and Catalán, P. A.: Source of the 1730 Chilean earthquake from historical records: Implications for the future tsunami hazard on the coast of Metropolitan Chile, J. Geophys. Res. Solid Earth, 122(5), 3648–3660, doi:10.1002/2017JB014063, 2017.

Cutter, S., Barnes, L., Berry, M., Burton, C., Evans, E., Tate, E. and Webb, J.: A place-based model for understanding community resilience to natural disasters, Glob. Environ. Chang., 18(4), 598–606, 2008.

Dewi, R. S.: A-Gis Based Approach of an Evacuation Model for Tsunami Risk Reduction, J. Integr. Disaster Risk Manag., 2(2), 2012.

Dill, J.: Measuring network connectivity for bicycling and walking, in 83rd Annual Meeting of the Transportation Research Board, Washington, DC., 2004.

Drápela, J., Calisto, I. and Moreno, M.: Locking-derived tsunami scenarios for the most recent megathrust earthquakes in Chile: implications for tsunami hazard assessment, Nat. Hazards 2021 1071, 107(1), 35–52, doi:10.1007/S11069-021-04572-5, 2021.

Eckert, S., Jelinek, R., Zeug, G. and Krausmann, E.: Remote sensing-based assessment of tsunami vulnerability and risk in Alexandria, Egypt, Appl. Geogr., 32(2), 714–723, doi:10.1016/J.APGEOG.2011.08.003, 2012.

Fakhrurrazi, F. and Van Nes, A.: Space and Panic. The application of Space Syntax to understand the relationship between mortality rates and spatial configuration in Banda Aceh during the tsunami 2004, in Eighth International Space Syntax Symposium, Santiago., 2012.

Frazier, T. G., Thompson, C. M. and Dezzani, R. J.: A framework for the development of the SERV model: A Spatially Explicit Resilience-Vulnerability model, Appl. Geogr., 51, 158–172, doi:10.1016/J.APGEOG.2014.04.004, 2014.

Fujii, Y. and Satake, K.: Slip Distribution and Seismic Moment of the 2010 and 1960 Chilean Earthquakes Inferred from Tsunami Waveforms and Coastal Geodetic Data, Pure Appl. Geophys. 2012 1709, 170(9), 1493–1509, doi:10.1007/S00024-012-0524-2, 2012.

González-Riancho Calzada, P., Aguirre Ayerbe, I., Aniel-Quiroga Zorrilla, Í., Abad Herrero, S., González Rodríguez, E. M., Larreynaga, J., Gavidia Medina, F., Gutiérrez Gutiérrez, O. Q., Álvarez Gómez, J. A. and Medina Santamaría, R.: Tsunami evacuation modelling as a tool for risk reduction: application to the coastal area of El Salvador, Nat. Hazards Earth Syst. Sci., 13, 3249–3270, 2013.

González-Riancho, P., Aliaga, B., Hettiarachchi, S., González, M. and Medina, R.: A contribution to the selection of tsunami human vulnerability indicators: conclusions from tsunami impacts in Sri and Japan (2011), Hazards Earth Syst. Sci, 15, 1493–1514, doi:10.5194/nhess-15-1493-2015, 2015.

Goto, Y. and Nakasu, T.: Human vulnerability index for evaluating tsunami evacuation capability of communities, J. Japan Assoc. Earthq. Eng., 18(6) [online] Available from: https://www.jstage.jst.go.jp/article/jaee/18/6/18_6_1/_article/-char/ja/ (Accessed 31 August 2021), 2018.

Handy, S., Paterson, R. G. and Butler, K.: Planning for Street Connectivity: Getting from Here to There, American Planning Association, Chicago., 2003.

Hillier, B.: Studying cities to learn about minds: some possible implications of space syntax for spatial cognition, Environ. Plan. B, 39(1), 12–32, 2009.

Hillier, B. and Iida, S.: Network effects and psychological effects: a theory of urban movement, 5th Int. Sp. Syntax Symp., 2005.

Imamura, F., Muhari, A., Mas, E., Pradono, M. H., Post, J. and Sugimoto, M.: Tsunami Disaster Mitigation by Integrating Comprehensive Countermeasures in Padang City, Indonesia, J. Disaster Res., 7(1), 48–64, 2012.

INE: Censo 2017, 2018.

INE: Porcentaje de población expuesta a inundación por tsunami, [online] Available from: https://insights.arcgis.com/#/embed/445a814f141a4b099a656a459bb7ce3d (Accessed 8 September 2021), 2021.

Kitamura, F., Inazu, D., Ikeya, T. and Okayasu, A.: An allocating method of tsunami evacuation routes and refuges for minimising expected casualties, Int. J. Disaster Risk Reduct., 45, 101519, doi:10.1016/j.ijdrr.2020.101519, 2020.

Klein, E., Vigny, C., Fleitout, L., Grandin, R., Jolivet, R., Rivera, E. and Métois, M.: A comprehensive analysis of the Illapel 2015 Mw8.3earthquake from GPS and InSAR data, Earth Planet. Sci. Lett., 469, 123–133, 2017.

Koshimura, S., Oie, T., Yanagisawa, H. and Imamura, F.: Developing Fragility Functions for Tsunami Damage Estimation Using Numerical Model and Post-Tsunami Data from Banda Aceh, Indonesia, Coast. Eng. J., 51(3), 243–273, doi:10.1142/S0578563409002004, 2009.

Kubisch, S., Guth, J., Keller, S., Bull, M. T., Keller, L. and Braun, A. C.: The contribution of tsunami evacuation analysis to evacuation planning in Chile: Applying a multi-perspective research design, Int. J. Disaster Risk Reduct., 45, 101462, doi:10.1016/j.ijdrr.2019.101462, 2020.

Lagos, M. and Gutiérrez, D.: Simulación del tsunami de 1960 en un estuario del centro-sur de Chile, Rev. Geogr. Norte Gd., 33, 5–18 [online] Available from: https://www.redalyc.org/pdf/300/30003301.pdf (Accessed 8 September 2021), 2005.

León, J., Mokrani, C., Catalán, P., Cienfuegos, R. and Femenías, C.: The role of built environment's physical urban form in supporting rapid tsunami evacuations: Using computer-based models and real-world data as examination tools, Front. Built Environ., 4, doi:10.3389/fbuil.2018.00089, 2019a.

León, J., Mokrani, C., Catalán, P., Cienfuegos, R. and Femenías, C.: The Role of Built Environment's Physical Urban Form in Supporting Rapid Tsunami Evacuations: Using Computer-Based Models and Real-World Data as Examination Tools, Front. Built Environ., 4, doi:10.3389/fbuil.2018.00089, 2019b.

León, J., Castro, S., Mokrani, C. and Gubler, A.: Tsunami evacuation analysis in the urban built environment: a multi-scale perspective through two modeling approaches in Viña del Mar, Chile, Coast. Eng. J., doi:10.1080/21664250.2020.1738073, 2020.

León, J., Vicuña, M., Ogueda, A., Guzmán, S., Gubler, A. and Mokrani, C.: From urban form analysis to metrics for enhancing tsunami evacuation: Lessons from twelve Chilean cities, Int. J. Disaster Risk Reduct., 58, 102215, doi:10.1016/j.ijdrr.2021.102215, 2021.

Løvholt, F., Setiadi, N. J., Birkmann, J., Harbitz, C. B., Bach, C., Fernando, N., Kaiser, G. and Nadim, F.: Tsunami risk reduction – are we better prepared today than in 2004?, Int. J. Disaster Risk Reduct., 10, 127–142, doi:10.1016/j.ijdrr.2014.07.008, 2014.

Lundberg, S. M.: SHAP (SHapley Additive exPlanations), [online] Available from: https://github.com/slundberg/shap (Accessed 11 January 2021), 2020.

Lundberg, S. M. and Lee, S.-I.: A Unified Approach to Interpreting Model Predictions, in Advances in Neural Information Processing Systems 30, pp. 4765–4774, Long Beach, CA. [online] Available from: https://github.com/slundberg/shap

(Accessed 15 October 2020), 2017.

Makinoshima, F., Imamura, F. and Abe, Y.: Behavior from Tsunami Recorded in the Multimedia Sources at Kesennuma City in the 2011 Tohoku Tsunami and Its Simulation by Using the Evacuation Model with Pedestrian—Car Interaction, Coast. Eng. J., 58(4), 1–28, 2016.

Marín Maureira, V. and Karimi, K.: The everyday and the post-disaster urban systems as one thing. A configurational approach to enchance the recovery and resilience of cities affected by tsunamis, in Proceedings of the 11th Space Syntax Symposium, Lisbon., 2017.

Mas, E., Koshimura, S., Suppasri, A., Matsuoka, M., Matsuyama, M., Yoshii, T., Jimenez, C., Yamazaki, F. and Imamura, F.: Developing Tsunami fragility curves using remote sensing and survey data of the 2010 Chilean Tsunami in Dichato, Nat. Hazards Earth Syst. Sci., 12(8), 2689–2697, doi:10.5194/NHESS-12-2689-2012, 2012.

Mas, E., Koshimura, S., Imamura, F., Suppasri, A., Muhari, A. and Adriano, B.: Recent Advances in Agent-Based Tsunami Evacuation Simulations: Case Studies in Indonesia, Thailand, Japan and Peru, Pure Appl. Geophys., 172(12), 3409–3424, doi:10.1007/s00024-015-1105-y, 2015.

Mas, E., Paulik, R., Pakoksung, K., Adriano, B., Moya, L., Suppasri, A., Muhari, A., Khomarudin, R., Yokoya, N., Matsuoka, M. and Koshimura, S.: Characteristics of Tsunami Fragility Functions Developed Using Different Sources of Damage Data from the 2018 Sulawesi Earthquake and Tsunami, Pure Appl. Geophys. 2020 1776, 177(6), 2437–2455, doi:10.1007/S00024-020-02501-4, 2020.

McKinney, W., Van den Bossche, J., Augspurger, T., Hoyer, S., Reback, J. and Cloud, P.: pandas, [online] Available from: https://pandas.pydata.org/ (Accessed 11 January 2021), 2020.

Medina, M., Riquelme, S., Fuentes, M. and Campos, J.: Tsunami Modeling in the South American Subduction Zone Inferred from Seismic Coupling and Historical Seismicity, Pure Appl. Geophys. 2021, 1–25, doi:10.1007/S00024-021-02808-W, 2021.

Mohareb, N. I.: Emergency evacuation model: accessibility as a starting point, Proc. Inst. Civ. Eng. Urban Des. Planning., 164(4), 215–224, 2011.

Mostafizi, A., Wang, H., Cox, D., Cramer, L. A. and Dong, S.: Agent-based tsunami evacuation modeling of unplanned network disruptions for evidence-driven resource allocation and retrofitting strategies, Nat. Hazards, 88(3), 1347–1372, doi:10.1007/s11069-017-2927-y, 2017.

Mostafizi, A., Wang, H., Cox, D. and Dong, S.: An agent-based vertical evacuation model for a near-field tsunami: Choice behavior, logical shelter locations, and life safety, Int. J. Disaster Risk Reduct., 34, 467–479 [online] Available from: https://www.sciencedirect.com/science/article/pii/S221242091830918X (Accessed 11 May 2020), 2019.

Mosteller, F. and Tukey, J. .: Data analysis, including statistics, in Handbook of Social Psychology, edited by G. Lindzey and E. Aronson, Addison-Wesley Pub. Co., Reading, Mass., 1968.

Murakami, H., Takimoto, K. and Pomonis, A.: Tsunami Evacuation Process and Human Loss Distribution in the 2011 Great East Japan Earthquake - A Case Study of Natori City, Miyagi Prefecture, in 15 WCEE, Lisbon., 2012.

https://doi.org/10.5194/nhess-2021-309
Preprint. Discussion started: 9 November 2021
© Author(s) 2021. CC BY 4.0 License.

Murray-Tuite, P. and Wolshon, B.: Evacuation transportation modeling: An overview of research, development, and practice, Transp. Res. Part C Emerg. Technol., 27, 25–45, doi:10.1016/J.TRC.2012.11.005, 2013.

Nateghi, R., Bricker, J. D., Guikema, S. D. and Bessho, A.: Statistical Analysis of the Effectiveness of Seawalls and Coastal Forests in Mitigating Tsunami Impacts in Iwate and Miyagi Prefectures, PLoS One, 11(8), e0158375, doi:10.1371/JOURNAL.PONE.0158375, 2016.

ONEMI: Recomendaciones para la preparación y respuesta ante tsunamis, ONEMI, Santiago, Chile., 2014.

Papazachos, B., Scordilis, E., Panagiotopoulos, D., Papazachos, C. and Karakaisis, G.: GLOBAL RELATIONS BETWEEN SEISMIC FAULT PARAMETERS AND MOMENT MAGNITUDE OF EARTHQUAKES, Bull. Geol. Soc. Greece, 36(3), 1482–1489, doi:10.12681/bgsg.16538, 2004.

Perry, R. W., Lindell, M. K. and Greene, M. R.: Evacuation Planning in Emergency Management, Lexington Books, Lexington, Massachusetts., 1981.

Porta, S., Crucitti, P. and Latora, V.: The Network Analysis of Urban Streets: A Primal Approach, Environ. Plan. B Plan. Des., 33(5), 705–725, doi:10.1068/b32045, 2006.

Sasabe, M., Fujii, K. and Kasahara, S.: Road network risk analysis considering people flow under ordinary and evacuation situations, Environ. Plan. B Urban Anal. City Sci., 47(5), doi:10.1177/2399808318802940, 2020.

SECTRA: Encuestas de Movilidad de Centros Urbanos, , (12-01–2014) [online] Available from: http://sintia.sectra.gob.cl/, 2014.

SECTRA: Encuesta de Origen-Destino de Viajes Gran Valparaíso, Ministerio de Obras Públicas, Transportes y Telecomunicaciones, Santiago, Chile., 2016.

Sevtsuk, A., Mekonnen, M. and Kalvo, R.: Urban Network Analysis. Toolbox for ArcGIS 10 / 10.1 / 10.2, City Form Lab, Singapore University of Technology & Design in collaboration with MIT, Singapore., 2013.

Sharifi, A.: Resilient urban forms: A review of literature on streets and street networks, Build. Environ., 147, 171–187, 2019.

SHOA: Proyecto CITSU, , (08-06–2012) [online] Available from: http://www.shoa.cl/index.htm, 2012.

Shuto, N.: Tsunamis: Their Coastal Effects and Defense Works, in Scientific Forum on the Tsunami, its Impact and Recovery, edited by T. Tingsanchali, pp. 1–12, Asian Institute of Technology, Bangkok, Thailand., 2005.

Sugimoto, T., Murakami, H., Kozuki, Y. and Nishikawa, K.: A Human Damage Prediction Method for Tsunami Disasters Incorporating Evacuation Activities, Nat. Hazards, (29), 585–600, 2003.

Suppasri, A., Mas, E., Charvet, I., Gunasekera, R., Imai, K., Fukutani, Y., Abe, Y. and Imamura, F.: Building damage characteristics based on surveyed data and fragility curves of the 2011 Great East Japan tsunami, Nat. Hazards, 66, 319–341, 2012a.

Suppasri, A., Shuto, N., Imamura, F., Koshimura, S., Mas, E. and Yalciner, A. C.: Lessons learned from the 2011 Great East Japan tsunami: Performance of tsunami countermeasures, coastal buildings, and tsunami evacuation in Japan, Pure Appl. Geophys., 170(6–8), 993–1018, 2012b.

Suppasri, A., Hasegawa, N., Makinoshima, F., Imamura, F., Latcharote, P. and Day, S.: An Analysis of Fatality Ratios and

https://doi.org/10.5194/nhess-2021-309
Preprint. Discussion started: 9 November 2021
© Author(s) 2021. CC BY 4.0 License.
Natural Hazards and Earth System Sciences
Discussions

the Factors That Affected Human Fatalities in the 2011 Great East Japan Tsunami, Front. Built Environ., 2, 32, doi:10.3389/fbuil.2016.00032, 2016.

Tarbotton, C., Dall'osso, F., Dominey-Howes, D. and Goff, J.: The use of empirical vulnerability functions to assess the response of buildings to tsunami impact: Comparative review and summary of best practice, Earth-Science Rev., 142, 120–134, 2015.

Taubenböck, H., Goseberg, N., Setiadi, N., Lämmel, G., Moder, F., Oczipka, M., Klüpfel, H., Wahl, R., Schlurmann, T., Strunz, G., Birkmann, J., Nagel, K., Siegert, F., Lehmann, F., Dech, S., Gress, A. and Klein, R.: "Last-Mile" preparation for a potential disaster - Interdisciplinary approach towards tsunami early warning and an evacuation information system for the coastal city of Padang, Indonesia, Nat. Hazards Earth Syst. Sci., 9, 1509–1528, doi:http://dx.doi.org/10.5194/nhess-9-1509-2009, 2009.

Ting, Y., Khew, J., Jarzebski, P., Dyah, F., Carlos, R. S., Gu, J., Esteban, M., Aránguiz, R. and Akiyama, T.: Assessment of social perception on the contribution of hard-infrastructure for tsunami mitigation to coastal community resilience after the 2010 tsunami: Greater Concepcion area, Chile, Int. J. Disaster Risk Reduct., 13, 324–333, doi:10.1016/j.ijdrr.2015.07.013, 2015.

Tobler, W.: Three presentations on geographical analysis and modeling: Non-isotropic geographic modeling; Speculations on the geometry of geography; and Global spatial analysis, NATIONAL CENTER FOR GEOGRAPHIC INFORMATION AND ANALYSIS, Santa Barbara, CA., 1993.

Tomita, T., Honda, K., Public, T. K.-T. M. of and 2006, U.: Application of storm surge and tsunami simulator in ocean and coastal areas (STOC) to tsunami analysis, pwri.go.jp [online] Available from: https://www.pwri.go.jp/eng/ujnr/joint/38/paper/38-41tomita.pdf (Accessed 9 March 2018), 2006.

Tsimopoulou, V., Jonkman, S. N., Kolen, B., Maaskant, B., Mori, N. and Yasuda, T.: A multi-layered safety perspective on the tsunami disaster in Tohoku, Japan, in FLOODrisk 2012: The 2nd European Conference on FLOODrisk Management, Rotterdam, NL., 2012.

Tumini, I., Villagra-Islas, P., Herrmann-Lunecke, G. and Cl, G. H.: Evaluating reconstruction effects on urban resilience: a comparison between two Chilean tsunami-prone cities, Nat. Hazards, 85, 1363–1392, doi:10.1007/s11069-016-2630-4, 2017.

Turner, A.: From Axial to Road-Centre Lines: A New Representation for Space Syntax and a New Model of Route Choice for Transport Network Analysis, Environ. Plan. B Plan. Des., 34(3), 539–555, doi:10.1068/b32067, 2007.

Turner, B. L., Kasperson, R. E., Matson, P. A., McCarthy, J. J., Corell, R. W., Christensen, L., Eckley, N., Kasperson, J. X., Luers, A. and Martello, M. L.: A framework for vulnerability analysis in sustainability science, Proc. Natl. Acad. Sci., 100(14), 8074–8079, 2003.

UNISDR: Terminology on Disaster Risk Reduction, [online] Available from: http://www.unisdr.org/files/7817_UNISDRTerminologyEnglish.pdf, 2009.

Villagra, P. and Quintana, C.: Disaster Governance for Community Resilience in Coastal Towns: Chilean Case Studies, Int.

https://doi.org/10.5194/nhess-2021-309
Preprint. Discussion started: 9 November 2021
© Author(s) 2021. CC BY 4.0 License.

J. Environ. Res. Public Heal. 2017, Vol. 14, Page 1063, 14(9), 1063, doi:10.3390/IJERPH14091063, 2017.

Villagra, P., Rojas, C., Ohno, R., Xue, M. and Gómez, K.: A GIS-base exploration of the relationships between open space systems and urban form for the adaptive capacity of cities after an earthquake: The cases of two Chilean cities, Appl. Geogr., 48, 64–78, doi:10.1016/j.apgeog.2014.01.010, 2014.

Wang, H., Mostafizi, A., Cramer, L. A., Cox, D. and Park, H.: An agent-based model of a multimodal near-field tsunami evacuation: Decision-making and life safety, Transp. Res. Part C Emerg. Technol., 64, 86–100, doi:10.1016/J.TRC.2015.11.010, 2016.

Wang, Z. and Jia, G.: A novel agent-based model for tsunami evacuation simulation and risk assessment, Nat. Hazards, 105(2), 2045–2071, doi:10.1007/S11069-020-04389-8, 2020.

WHO: Tsunamis, [online] Available from: https://www.who.int/health-topics/tsunamis#tab=tab_1 (Accessed 12 August 2021), 2021.

Wisner, B., Gaillard, J. C. and Kelman, I.: Framing disaster. Theories and stories seeking to understand hazards, vulnerability and risk, in The Routledge Handbook of Hazards and Disaster Risk Reduction, edited by B. Wisner, J. C. Gaillard, and I. Kelman, pp. 18–33, Routledge, Oxon, UK., 2012.

Wood, N., Jones, J., Schelling, J. and Schmidtlein, M.: Tsunami vertical-evacuation planning in the US Pacific Northwest as a geospatial, multi-criteria decision problem, Int. J. Disaster Risk Reduct., 9, 68–83, 2014.

Wood, N., Jones, J. M., Yamazaki, Y., Kwok-Fai, C., Brown, J., Jones, J. L. and Abdollahian, N.: Population vulnerability to tsunami hazards informed by previous and projected disasters: a case study of American Samoa, Nat. Hazards, 95(3), 505–528, doi:10.1007/s11069-018-3493-7, 2018.

Wood, N., Peters, J., Wilson, R., Sherba, J. and Henry, K.: Variations in community evacuation potential related to average return periods in probabilistic tsunami hazard analysis, Int. J. Disaster Risk Reduct., 50, 101871, doi:10.1016/j.ijdrr.2020.101871, 2020.

Yao, J., Lin, C., Xie, X., Wang, A. J. and Hung, C.-C.: Path Planning for Virtual Human Motion Using Improved A* Star Algorithm, in 2010 Seventh International Conference on Information Technology: New Generations, edited by S. Latifi, pp. 1154–1158, IEEE, Las Vegas, NV., 2010.

Yavuz, C., Kentel, E. and Aral, M. M.: Tsunami risk assessment: economic, environmental and social dimensions, Nat. Hazards, 104(2), 1413–1442, doi:10.1007/S11069-020-04226-Y, 2020.

Zamora, N., Catalán, P. A., Gubler, A. and Carvajal, M.: Microzoning Tsunami Hazard by Combining Flow Depths and Arrival Times, Front. Earth Sci., 8, 747, doi:10.3389/feart.2020.591514, 2021.